Sensors and Materials, Vol. 38, No. 2 (2026) 635–638
MYU Tokyo

S & M 4332

Radiation Response Properties of Sn-doped $BaO–P_2O_5$ Glasses Prepared by Melt-quenching Method

Keishi Yamabayashi,* Akihiro Nishikawa, Keiichiro Miyazaki, Kai Okazaki, Daisuke Nakauchi, Takumi Kato, Noriaki Kawaguchi, and Takayuki Yanagida

Nara Institute of Science and Technology (NAIST), 8916-5 Takayama-Cho, Ikoma, Nara 630-0192, Japan

(Received October 30, 2025; accepted December 9, 2025)

Keywords: scintillation, phosphate glass, photoluminescence, α-rays

Sn-doped $50BaO–50P_2O_5$ glasses were synthesized by the melt-quenching method, and their radiation response properties were evaluated. In both photoluminescence (PL) and scintillation, all the samples showed broad emission peaks at around 450 nm owing to the $T_1–S_0$ transition of Sn^{2+}. Among the samples, the highest PL quantum yield (31.3%) and light yield (240 ph/5.5 MeV-α) were obtained in the 1% Sn-doped sample.

1. Introduction

Scintillators convert high-energy ionizing radiations such as X- and γ-rays into low-energy photons, which are extensively utilized in medical imaging,[1] security inspection,[2] and high-energy physics.[3] For these applications, scintillators are required to show high light yield (*LY*), fast decay, large effective atomic number (Z_{eff}), and high chemical stability. However, there is no material that meets all the requirements. Thus, various types of scintillator, including single crystals,[4–8] ceramics,[9–12] and glasses,[13–15] have been developed to satisfy each demand.

Glasses are particularly attractive as scintillators because of their low production cost, excellent processability, and high compositional flexibility. These features make it possible to fabricate large, optically uniform samples for fundamental research through conventional melt-quenching processes without complex and expensive fabrication techniques. Owing to these advantages, various glasses such as silicate,[16,17] borate,[18,19] and phosphate[20,21] have been proposed for radiation detection.

Here, we focused on phosphate glasses, which can be fabricated at temperatures lower than those of other glass systems. The glass host is the $BaO–P_2O_5$ system, which forms a flexible phosphate network mainly composed of interconnected PO_4 tetrahedra.[22] BaO strengthens the network by bonding with non-bridging oxygen and increases Z_{eff}.[23] As an emission center, Sn^{2+} was selected owing to its high photoluminescence (PL) and scintillation intensities reported in various glass hosts such as SiO_2 (~1650 ph/5.5 MeV-α)[17] and $HfO_2–Al_2O_3–SiO_2$ (~2500 ph/5.5 MeV-α).[24] In this study, Sn-doped $50BaO–50P_2O_5$ glasses were synthesized by the conventional melt-quenching method, and their PL and radiation response properties were investigated.

*Corresponding author: e-mail: yamabayashi.keishi.yh2@ms.naist.jp
https://doi.org/10.18494/SAM6014

ISSN 0914-4935
https://myukk.org/

2. Experimental Methods

The 50BaO–50P_2O_5 glasses with Sn concentrations of 0.3, 1, and 3 mol% were fabricated by the conventional melt-quenching method. $BaCO_3$ (4N), $NH_4H_2PO_4$ (4N), and SnO_2 (4N) powders were used as starting materials. The powders, with a total amount of 1 g, were weighed at each molar ratio and mixed using an agate mortar. The mixture was put into alumina crucibles and heated at 1200 °C for 2 h in an atmospheric environment. The melts were poured onto a hot plate kept at 400 °C and rapidly quenched by pressing with stainless plates. The obtained glasses, ~0.5 cm^2 in size, were collected and polished for each measurement.

The powder X-ray diffraction pattern (PXRD) was measured with a diffractometer (Rigaku, MiniFlex600). The PL excitation/emission mapping and PL*QY* were evaluated with Quantaurus-QY (Hamamatsu Photonics, C11347). The PL decay curves were measured using Quantaurus-τ (Hamamatsu Photonics, C11367). The X-ray-induced scintillation and pulse height spectra were collected using our original setups.[25]

3. Results and Discussion

Figure 1(a) shows the appearances and PXRD patterns of the samples. All the samples were colorless and transparent, and no crystalline phases were detected in the PXRD patterns, confirming that the samples were amorphous. Figure 1(b) shows the PL excitation/emission mapping of the 1% Sn-doped sample and the PL decay curves of the samples, since all the samples exhibited similar behaviors. The emission intensity is normalized to the maximum signal, and the regions of highest and lowest intensities are shown in white and black, respectively. Broad emission peaks at 350–700 nm were observed under excitation at 250–325 nm. The PL*QY* values of 0.3, 1, and 3% Sn-doped samples under excitation at 280 nm were 5.0, 31.3, and 9.6%, respectively. Concentration quenching was observed at the 3% Sn-doped sample. From the mapping results, the PL decay curve monitored at 450 nm was measured under excitation at 280 nm. All the obtained PL decay curves were well approximated by a single exponential function. The decay time constants of the 0.3, 1, and 3% Sn-doped samples were calculated to be 6.2, 6.9, and 6.6 μs, respectively. The constants were almost equivalent to those

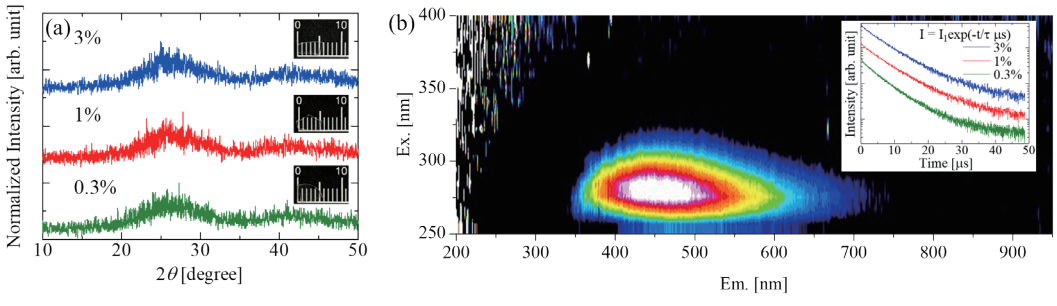

(a) (b)

Fig. 1. (Color online) (a) Appearances and PXRD patterns (scale bar = 1 mm) of the samples, (b) PL excitation/emission mapping of the 1% Sn-doped sample and PL decay curves of the samples.

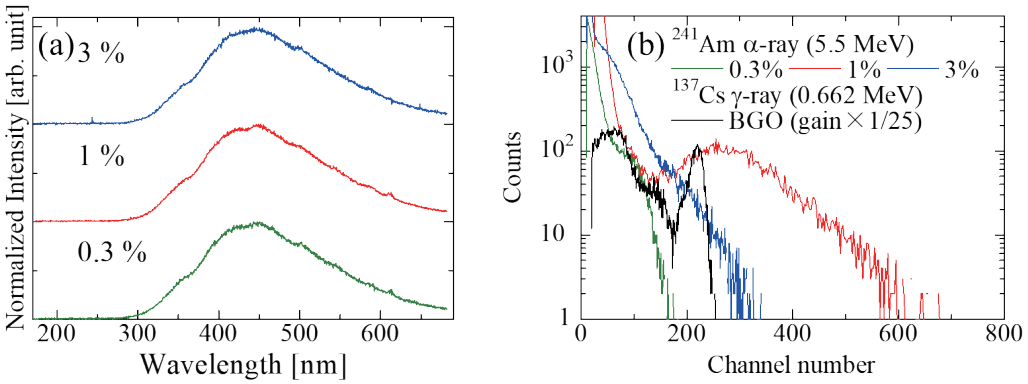

Fig. 2. (Color online) (a) X-ray-induced scintillation and (b) pulse height spectra of the samples.

of Sn-doped glasses reported previously; thus, the origin of PL was ascribed to the T_1–S_0 transition of Sn^{2+}.[17, 24]

Figure 2(a) shows the X-ray-induced scintillation spectra of the samples. Broad emission peaks were observed at around 450 nm, and the spectral shapes were the same as that in PL. Thus, the origin of scintillation was ascribed to the T_1–S_0 transition of Sn^{2+}. Figure 2(b) shows the pulse height spectra of ^{241}Am α-rays (5.5 MeV) measured using the samples to calculate *LY*s. For the calculation, the *LY* of $Bi_4Ge_3O_{12}$ (BGO: 8000 ph/MeV[26]) under irradiation with ^{137}Cs γ-rays (0.662 MeV) was used as a reference. *LY*s were calculated using the following equation: $LY_{sample} = LY_{ref} \times E \times (channel_{sample}/channel_{ref}) \times (QE_{ref}/QE_{sample})$, where E is the γ-ray energy, channel shows the position of full energy or photoabsorption peaks, and *QE* denotes the quantum efficiency of the photomultiplier (R7600-200, Hamamatsu Photonics) The *QE* values of the samples and BGO were 24.93 and 21.18%, respectively . The peak channels were evaluated by a single Gaussian fitting, and the obtained channels for the 0.3, 1, and 3% Sn-doped samples were 100, 290, and 200 ch, respectively. The *LY* values of the 0.3, 1, and 3% Sn-doped samples were calculated to be 80, 240, and 180 ph/5.5 MeV-α, respectively. The highest *LY* among the samples (240 ph/5.5 MeV-α) was lower than those of other Sn-doped glasses such as 0.5% Sn-doped SiO_2 (~1650 ph/5.5 MeV-α[17]) and 1.0% Sn-doped $10HfO_2$–$10Al_2O_3$–$80SiO_2$ (~2500 ph/5.5 MeV-α[24]). According to the simplified model proposed by Robbins,[27] *LY* is proportional to $S \times QY$, where S represents the energy transfer efficiency. In this study, the *LY* of the samples showed a clear correlation with *QY*, which is consistent with Robbins' model.

4. Conclusions

Sn-doped $50BaO$–P_2O_5 glasses were successfully prepared by the melt-quenching method, and their PL and scintillation properties were investigated. Both in PL and scintillation, broad emission peaks derived from the T_1–S_0 transition of Sn^{2+} were observed. In the 1% Sn-doped sample, the highest *LY* among the samples was obtained (240 ph/5.5 MeV-α), and the trend of *LY* was consistent with Robbins' model. To further increase *LY*, additional investigations on the glass composition or synthesis conditions are required.

Acknowledgments

This work was supported by JSPS KAKENHI (Grant nos. 22H00309, 23K25126, 24K03197, 23K13689, and 25K08266), the Cooperative Research Project of the Research Center for Biomedical Engineering, JSPS Fellows (25KJ1820), and Shimadzu Science Foundation.

References

1 A. Nassalski, M. Kapusta, T. Batsch, D. Wolski, D. Möckel, W. Enghardt, and M. Moszyński: IEEE Trans. Nucl. Sci. **5** (2005) 2823.
2 F. Zhou, Z. Li, W. Lan, Q. Wang, L. Ding, Z. Jin, F. Zhou, Z. Li, W. Lan, Q. Wang, Z. Jin, and L. Ding: Small Methods **4** (2020) 2000506.
3 G. I. Britvich, V. V. Brekhovskikh, V. K. Semenov, and S. A. Kholodenko: Instrum. Exp. Tech. **58** (2015) 211.
4 M. Koshimizu: Jpn. J. Appl. Phys. **62** (2022) 010503.
5 K. Miyazaki, D. Nakauchi, T. Kato, N. Kawaguchi, and T. Yanagida: Sens. Mater. **36** (2024) 515.
6 H. Fukushima, D. Nakauchi, T. Kato, N. Kawaguchi, and T. Yanagida: Sens. Mater. **36** (2024) 489.
7 H. Kimura, H. Fukushima, K. Watanabe, T. Fujiwara, H. Kato, M. Tanaka, T. Kato, D. Nakauchi, N. Kawaguchi, and T. Yanagida: Sens. Mater. **36** (2024) 507.
8 K. Miyazaki, D. Nakauchi, Y. Takebuchi, T. Kato, N. Kawaguchi, and T. Yanagida: Sens. Mater. **37** (2025) 575.
9 T. Kato, D. Nakauchi, N. Kawaguchi, and T. Yanagida: Sens. Mater. **36** (2024) 531.
10 D. Shiratori, H. Kimura, Y. Fukuchi, and T. Yanagida: Sens. Mater. **36** (2024) 547.
11 S. Muneta, N. Kawano, D. Nakauchi, T. Kato, K. Okazaki, K. Ichiba, T. Kunikata, A. Nishikawa, K. Miyazaki, F. Kagaya, K. Shinozaki, and T. Yanagida: Sens. Mater. **37** (2025) 509.
12 S. Otake, S. Takase, T. Kato, D. Nakauchi, N. Kawaguchi, and T. Yanagida: Sens. Mater. **37** (2025) 519.
13 Y. Takebuchi, A. Masuno, D. Shiratori, K. Ichiba, A. Nishikawa, T. Kato, D. Nakauchi, N. Kawaguchi, and T. Yanagida: Sens. Mater. **36** (2024) 579.
14 K. Okazaki, D. Nakauchi, A. Nishikawa, T. Kato, N. Kawaguchi, and T. Yanagida: Sens. Mater. **36** (2024) 587.
15 H. Fukushima, R. Tsubouchi, T. Matsuura, T. Yoneda, and T. Yanagida: Sens. Mater. **37** (2025) 487.
16 A. Nishikawa, D. Shiratori, T. Kato, D. Nakauchi, N. Kawaguchi, and T. Yanagida: Sens. Mater. **36** (2024) 597.
17 D. Shiratori, H. Kimura, D. Nakauchi, T. Kato, N. Kawaguchi, and T. Yanagida: Radiat. Meas. **134** (2020) 106297.
18 H. Kawamoto, Y. Fujimoto, and K. Asai: Sens. Mater. **36** (2024) 607.
19 K. Miyajima, A. Nishikawa, T. Kato, D. Nakauchi, N. Kawaguchi, and T. Yanagida: Sens. Mater. **37** (2025) 481.
20 N. Wantana, E. Kaewnuam, Y. Tariwong, N. D. Quang, P. Pakawanit, C. Phoovasawat, N. Vittayakorn, S. Kothan, H. J. Kim, and J. Kaewkhao: Jpn. J. Appl. Phys. **62** (2023) 010602.
21 H. Kawamoto, M. Koshimizu, Y. Fujimoto, and K. Asai: Jpn. J. Appl. Phys. **62** (2022) 010501.
22 R. K. Brow: J. Non. Cryst. Solids **263–264** (2000) 1.
23 X. Wang, G. Zhou, H. Zhang, S. Du, Y. Xu, and C. Wang: J. Non-Cryst. Solids **357** (2011) 3027.
24 D. Shiratori, H. Fukushima, D. Nakauchi, T. Kato, N. Kawaguchi, and T. Yanagida: Jpn. J. Appl. Phys. **62** (2022) 010608.
25 T. Yanagida, K. Kamada, Y. Fujimoto, H. Yagi, and T. Yanagitani: Opt. Mater. **35** (2013) 2480.
26 M. Moszyński, M. Balcerzyk, W. Czarnacki, M. Kapusta, W. Klamra, A. Syntfeld, and M. Szawlowski: IEEE Nucl. Sci. **1** (2003) 92.
27 D. J. Robbins: J. Electrochem. Soc. **127** (1980) 2694.